

Cu DOPED Bi_2S_3 AS POTENTIAL ABSORBERS FOR THIN FILM SOLAR CELLS: OPTICAL AND STRUCTURAL PROPERTIES

T. FAZAL^a, B. ISMAIL^a, S. WAFEE^a, A. H. KAMBOOH^b, A. R. KHAN^{a*}

^a*Department of Chemistry, COMSATS Institute of Information Technology, Abbottabad 22060, Pakistan*

^b*Pakistan Council of Renewable Energy Technologies, PCRET, H-9, Islamabad 44000, Pakistan.*

Thin films of copper doped bismuth sulphide were deposited by chemical bath deposition technique onto glass substrate at room temperature. The set of films having different elemental compositions was prepared by varying Cu weight percent from 0.93-14.54. Deposition mechanism of Cu doped Bi_2S_3 chalcogenides has been discussed. Studies on structure, composition, morphology and optical absorption of the films were carried using X-ray diffraction (XRD), energy dispersive X-ray spectroscopic analysis (EDAX), scanning electron microscopy (SEM), atomic force microscopy (AFM), UV/Vis absorption spectroscopy. Optical band gap energy, E_g , in the range of 1.1 to 1.4, refractive index having the range 1.3 to 2.01 was observed for different Cu/Bi ratios.

(Received January 20, 2016; Accepted May 27, 2016)

Keywords: thin films; optical properties; doping; solar cells

1. Introduction

Current leaders in thin film solar cells [1] namely $\text{Cu}(\text{InGa})\text{Se}_2$ and CdTe -based devices have shown major success but due to their limited availability [2], large scale manufacturing cost and toxicity issues restricts their use to cope the escalating needs of photovoltaic industry. $\text{Cu}_2\text{ZnSn}(\text{SSe})_4$, has been investigated recently as an alternative and modified form of CuInSe_2 , where rare and expensive In/Ga are substituted with cheap and abundant Zn and Sn elements [3]. But the complexity of this compound i.e. very narrow single phase region in its phase diagram and hence susceptibility of presence of secondary phases in the material restricts its practical applications [4]. Metal chalcogenides have suitable electrical and optical properties and recently emerged as important class of materials for photovoltaic application.

Number of binary and ternary chalcogenide materials such as CdSe [5], CdS [6], $\text{CdS}_{1-x}\text{Se}_x$, ZnSe [7], ZnS , $\text{Zn}_{1-x}\text{Cd}_x\text{S}$, $\text{Cd}_{1-x}\text{Zn}_x\text{S}$ [8], Sb_2S_3 [9], Sb_2Se_3 [10], Bi_2Se_3 and Bi_2S_3 [11, 12] have been used as semiconductors in electrochemical photovoltaic cells. Bismuth sulphide is a promising semiconductor and its band gap energy lies in the range 1.2–1.7 eV. It has a reasonable incident photon to electron conversion efficiency of ~5%. The electrical resistivity of Bi_2S_3 is of the order of $10^4 \Omega\cdot\text{cm}$ and is useful in the conversion of solar energy into electrical energy [13].

Alteration of properties by the incorporation of other metals is a traditionally used method. More recently, it has been investigated that the doping by Cu has a reasonable effect on the structural, electrical as well as the optical properties [14]. These compounds have high absorption coefficient of $\sim 10^5 \text{cm}^{-1}$ [15] and direct band gap having values ranging from 1.14 [15] to 1.41 eV [16, 17]. But detailed exploration of properties of Cu doped Bi_2S_3 thin films needs more attention for their potential applications in thin film solar cells.

In the current study, thin films of Cu doped Bi_2S_3 have been deposited by an easy and cost effective chemical bath deposition technique. Room temperature deposition of doped thin films has been attempted to thoroughly investigate the morphological and optical properties.

* Corresponding authors: khanar@ciit.net.pk

2. Experimental

Bismuth nitrate ($\text{Bi}(\text{NO}_3)_3 \cdot 5\text{H}_2\text{O}$, BDH, 98%), copper nitrate ($\text{Cu}(\text{NO}_3)_2 \cdot 3\text{H}_2\text{O}$, BDH, 98%), thioacetamide (CH_3CSNH_2 , Aldrich, 99%) and ethylene diamine tetra acetic acid ($\text{C}_{10}\text{H}_{16}\text{N}_2\text{O}_8$, Sigma, 99%) were used as received for thin films deposition. The microscopic glass slides were used as substrates after cleaning. The cleaning was carried out by hot distilled water, ethyl alcohol, chromic acid and finally with distilled water. These slides were vacuum dried for 1hr at 100 °C. The bath was prepared by mixing a 10 ml of aqueous solution of 0.1M thioacetamide and 8 ml of 0.1 M aqueous solution of ethylene diaminetetra acetic acid (EDTA). The bath (10 ml) was prepared using 1%, 2%, 3%, 4% and 5% trihydrated copper nitrate solutions with respect to penta hydrated bismuth nitrate in an acidic medium (3M HNO_3). Both the solutions were mixed in equal ratios and stirred for 1-2 min. The deposition process involves the reaction of Cu^{2+} and/or Bi^{3+} ions with S^{2-} ions in deionized water solution. Films were deposited for 6 hrs at room temperature.

Phase composition and crystallinity of thin films were studied by X-ray diffraction (XRD) using PANalytical Xpert' Pro (Holland) diffractometer having monochromatic Cu-K_α radiation source ($\lambda=1.5418\text{\AA}$) at 40 KV and 30 mA in the 2θ range of $20-80^\circ$ with step size of 0.05° per minute. Surface morphologies of the thin films were studied by scanning electron microscope JEOL, JSM5910 Japan. An AFM nanoscope digital instrument with a silicon nitride cantilever was used to probe different portions of the film surface in "contact mode AFM". UV/Vis spectra were taken using the Perkin Elmer Lambda 25 spectrophotometer.

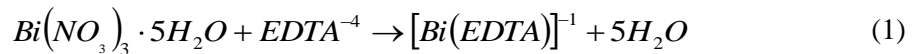
3. Results and Discussion

3.1 Mechanism of deposition of Cu doped Bi_2S_3 thin films deposition

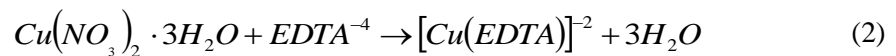
The deposition of Cu doped Bi_2S_3 follows the mechanism given below:

(i) Formation of metal complexes

Addition of EDTA to the aqueous solution of $\text{Bi}(\text{NO}_3)_3 \cdot 5\text{H}_2\text{O}$ results the formation of complexed species. Bismuth ions refrain hydrolysis in the presence of EDTA [18].

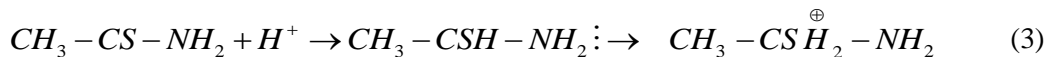


In a same way copper ions are complexed by EDTA.

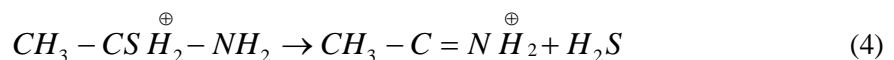


(ii) Dissociation of thioacetamide

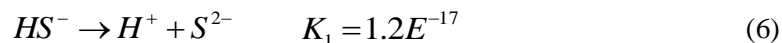
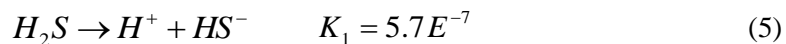
Thioacetamide in acidic medium undergoes following sequence of reactions [18], i.e. protonation and intermediate dissociation [19].



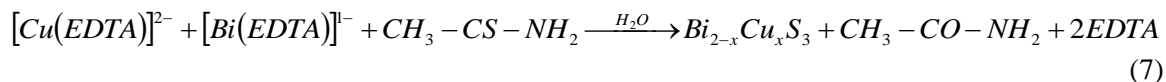
Finally, above intermediate dissociates into sulphide ion.



In aqueous medium, H_2S releases S^{2-} ion [19].



Consumption of S^{2-} by bismuth triggers the reaction in forward reaction. Overall reaction to form Cu doped Bi_2S_3 is as follows:



3.2 Morphological studies

The surface morphology of pure Bi_2S_3 and Cu doped thin films deposited by CBD is shown in Figs. 1(a-d). Fig. 1(a) reveals the morphology of pure Bi_2S_3 sample having homogenous and uniform particles. Increasing the dopant concentration (Figs. b-d having 1, 3 and 5% Cu, respectively) resulted in the reduced grain size compared to pure Bi_2S_3 , as well as better crystallinity. The grain size inncreased with the increasing dopant concentration.

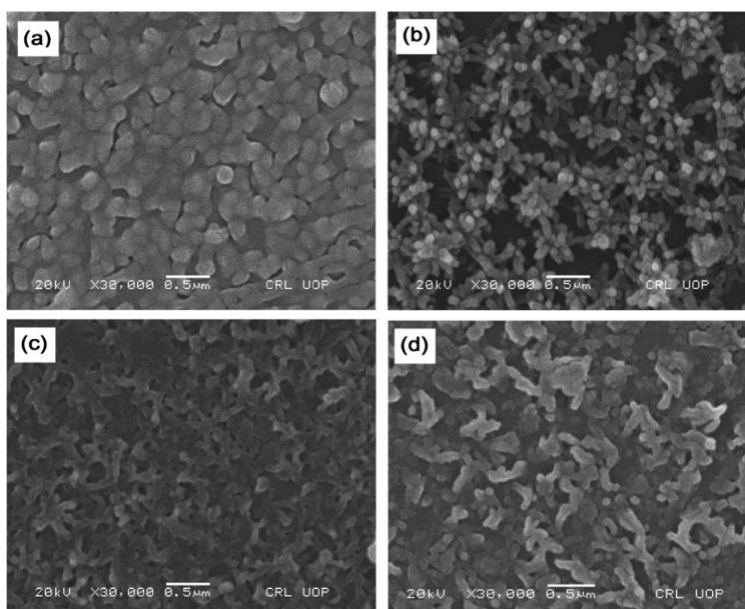


Fig.1. Scanning electron micrographs of the deposited thin films (a) Bi_2S_3 , (b) 1% Cu, (c) 3% Cu and (d) 5% Cu doped and $Bi_{2-x}Cu_xS_3$

Figs. 2(a-d) show the three dimensional AFM images of pure and Cu doped Bi_2S_3 thin films in a projected area of $10.0 \times 10.0 \mu m^2$. The pure Bi_2S_3 sample as shown in Fig. 2(a), has heighted and huge brailed structures. The particles have evident boundaries and shape In Fig. 2(b-c), with the increase of dopant concentration, the height of the structure, roughness and particle size is decreasing.

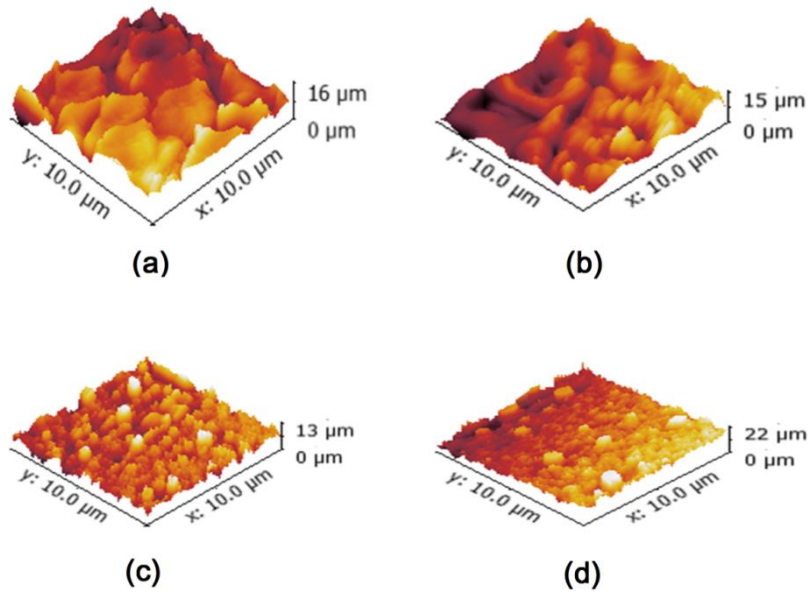


Fig. 2. Three dimensional AFM images of the deposited thin films of (a) Bi_2S_3 , (b) 1% Cu, (c) 3% Cu and (d) 5% Cu doped and $\text{Bi}_{2-x}\text{Cu}_x\text{S}_3$.

Table 1 shows the elemental composition of the films determined by EDX. Theoretically expected stoichiometric composition of Cu doped Bi_2S_3 in terms of at % is (Cu + Bi)=40% and S=60%. Cu/Bi ratios vary from 0.01-0.22.

Table 1. Experimental elemental composition of Bi_2S_3 and $\text{Bi}_{2-x}\text{Cu}_x\text{S}_3$ thin film materials

Sample Code	Wt. %				At. %			
	Bi	Cu	S	Cu/Bi	Bi	Cu	S	Cu/Bi
S	88.00	0.00	12.00	0.00	53.40	0.00	46.60	0.00
S1	87.89	0.93	11.90	0.01	52.36	1.85	45.79	0.03
S3	71.13	4.89	23.98	0.07	31.14	7.22	61.64	0.23
S5	63.40	14.54	22.06	0.22	24.34	18.86	56.80	0.71

X-Ray diffraction gives information regarding the evolution of the crystalline phases as a function of time and annealing temperature. Lattice parameters “a, b and c”, unit cell volume “ V_{cell} ”, Scherrer crystallite size “D” and X-ray density “ $\rho_{\text{x-ray}}$ ” were calculated using the equations 9-12.

$$\frac{1}{d^2} = \frac{h^2}{a^2} + \frac{k^2}{b^2} + \frac{l^2}{c^2} \quad (8)$$

$$V_{\text{cell}} = abc \quad (9)$$

$$D = \frac{k\lambda}{\beta \cos \theta_B} \quad (10)$$

$$\rho_{\text{x-ray}} = \frac{ZM}{V_{\text{cell}}N_A} \quad (11)$$

Where d is d -spacing of lines in XRD pattern, hkl are corresponding miller indices to each line in the pattern, β is the full width at half maximum of intensity, λ is the wavelength of CuK_α X-rays and is equal to 1.542 \AA , θ is the Bragg's angle and k is the constant, which is equal to 0.94, Z is the number of molecules per formula unit, M is the molar mass, V_{cell} and N_A have their usual meanings. Fig. 3 shows the XRD patterns of Bi_2S_3 and $\text{Bi}_{2-x}\text{Cu}_x\text{S}_3$ thin films. The presences of sharp and well-defined peaks in these patterns confirm the polycrystalline nature of the films. Comparison of the observed diffraction pattern with standard pattern (JCPDS Card No. 01-084-0279) reveals that the material belongs to bismuthinite phase of bismuth sulphide. For doped samples, shift in the diffraction angles is observed due to the fact that the lattice constant decreases with increasing zinc concentration with the addition of copper content in Bi_2S_3 , which is evidence of the complete transformation of binary compounds into ternary compounds after incorporation of aliovalent Cu. Crystallite size "D" and the intensity of the peaks were found to decrease with the addition of copper. This is acceptable because the atomic radius of Cu is less than the atomic radius of Bi.

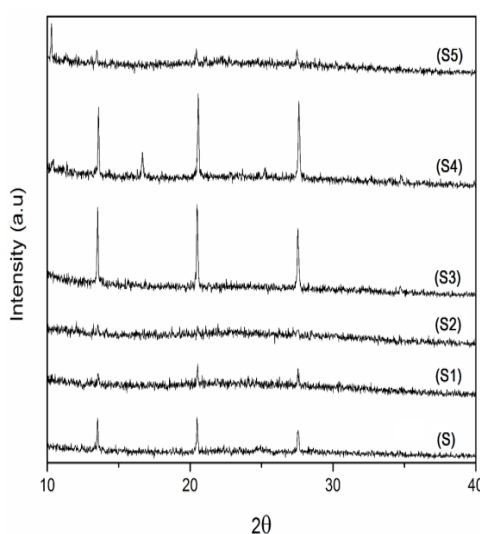


Fig.3. XRD patterns of (S) Bi_2S_3 , (S1) 1%, (S2) 2% (S3) 3% (S4) 4% and (S5) 5% Cu doped $\text{Bi}_{2-x}\text{Cu}_x\text{S}_3$

3.3 UV-Vis spectroscopy

The optical parameters for example, band gap, transmission, refractive index, and absorption coefficient are determined from the absorption studies on the films. The Tauc equation is given below which is used to calculate the band gaps of the deposited films:

$$(\alpha h\nu)^n = A(h\nu - E_g) \quad (12)$$

Where h is Planks constant, $h\nu$ is the energy of electromagnetic radiation, α is the absorption coefficient, E_g is the band gap and A is the proportionality constant. The value of exponent n can be 2, 2/3, 1/2 and 1/3 for the direct allowed, direct forbidden, indirect allowed and indirect forbidden transitions, respectively. The best fit to the experimental data is obtained for $n = 2$ and the corresponding direct allowed band gaps are given in Table 2. The band gap values are acceptable for the suitability of thin films as visible light absorber materials. Band gaps are found to be dependent on the crystallinity of the films, atomic/weight ratios of Bi and S and the deposition method[20].

Table 2: Comparison of the optical parameters of the deposited thin film samples

Parameters	Samples					
	S	S1	S2	S3	S4	S5
E_g (eV)	1.1	1.2	1.25	1.3	1.35	1.4
$\alpha \times 10^4$ (cm ⁻¹)	0.14	1.33	1.21	1.14	1.03	0.96
n	1.2	2.03	2.00	1.97	1.90	1.81
ϵ	1.68	4.22	4.03	3.89	3.62	3.49
$\sigma_e \times 10^3$ (Ω.cm) ⁻¹	6.81	9.03	7.48	8.82	0.11	11.0
$\sigma_o \times 10^{14}$ (s ⁻¹)	7.59	4.15	7.95	8.43	7.5	10.2
$\sigma_t \times 10^{-8}$ (W.m/K)	8.09	0.19	9.67	8.28	6.6	6.63

The variation of absorbance (A) is studied in the wavelength range of 400-800 nm for all the deposited samples. The UV/Vis spectra are shown in Fig. 4. The absorption coefficient is calculated from reflectance, transmittance and the thickness data of the thin film as given in the relations below:

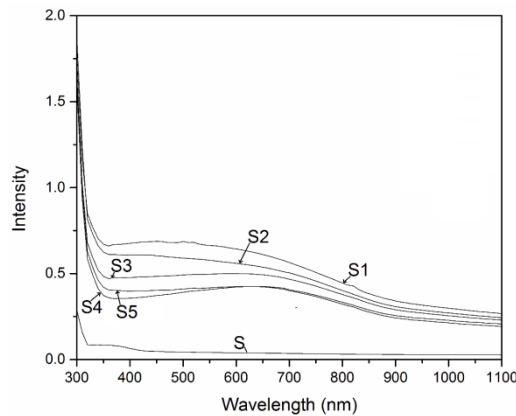
$$\alpha (cm^{-1}) = \frac{1}{d} \ln \frac{(1-R)^2}{T} \quad (13)$$

Transmittance and reflectance are calculated from the following relations[21]:

$$T = 10^{-A} \quad (14)$$

$$R = 1 - [T \exp(A)]^{1/2} \quad (15)$$

The values of absorption coefficient are given in **Table 2**. The values of the absorption coefficient obtained in this study are comparatively higher than the values reported in the literature. The high values of absorption coefficient validate their use in photovoltaic applications. Refractive index, dielectric constant, electrical conductivity, optical conductivity and thermal conductivity also show good values.

Fig.4. UV-visible spectra of Bi_2S_3 and $Bi_{2-x}Cu_xS_3$ thin films

4. Conclusions

Homogeneous and uniform copper doped bismuth sulphide films were deposited on to glass substrate by simple chemical bath deposition technique. The values of bandgap energy go on

increasing with the increase of Cu/Bi ratio. Optical bandgap energy, E_g , in the range of 1.1 to 1.4 and refractive index having the range 1.3 to 1.4 was observed for different Cu/Bi ratio. These changes are attributed to the quantum size effect in semiconducting films. AFM observations indicated that the films were relatively smooth and SEM depicted that particles were found to be arranged in a flower shape manner and EDX studies showed nonstoichiometric nature of thin films.

References

- [1] M.A. Geeny, K. Emery, Y. Hishikawa, W. Warta, *Progress in photovoltaics* **19**(1),84 (2011).
- [2] B.A. Andersson, *Progress in photovoltaics: research and applications* **8**(1)61 (2000).
- [3] F. Luckert, D. Hamilton, M. Yakushev, N. Beattie, G. Zoppi, M. Moynihan, I. Forbes, A. Karotki, A. Mudryi, M. Grossberg, *Applied Physics Letters* **99**(6),062104 (2011).
- [4] S. Siebentritt, S. Schorr, *Progress in Photovoltaics: Research and Applications* **20**(5),512 (2012).
- [5] M.A. Barote, A.A. Yadav, E.U. Masumdar, *Physica B: Condensed Matter* **406**(10),1865 (2011).
- [6] C.B. Roy, D.K. Nandi, P.K. Mahapatra, *Electrochimica Acta* **31**(10),1227 (1986).
- [7] P.P. Hankare, P.A. Chate, D.J. Sathe, *J Alloy Compd* **487**(1-2),367 (2009).
- [8] G.S. Shahane, K.M. Garadkar, L.P. Deshmukh, *Mater Chem Phys* **51**(3),246 (1997).
- [9] K.Y. Rajpure, C.H. Bhosale, *Mater Chem Phys* **64**(1)14 (2000).
- [10] P.B. Bagdare, S.B. Patil, A.K. Singh, *J Alloy Compd* **506**(1),120 (2010).
- [11] B. Bhattacharyya, P.K. Kalita, P. Datta, P.K. Giri, D.K. Goswami, A. Perumal, A. Chattopadhyay, *AIP Conference Proceedings* **1276**,124 (2010).
- [12] K.W. Böer, *Journal of Photochemistry* **10**(1),77 (1979).
- [13] M.E. Rincon, P.K. Nair, *Semiconductor Science and Technology* **12**(4),467 (1997).
- [14] V. Estrella, M.T.S. Nair, P.K. Nair, *Semiconductor Science and Technology* **18**(2),190 (2003).
- [15] F. Mesa, G. Gordillo, *Journal of Physics: Conference Series*, IOP Publishing, 2009, p. 012019.
- [16] M. Kumar, C. Persson, *Applied Physics Letters* **102**(6),062109 (2013).
- [17] C. Tablero, *Progress in Photovoltaics: Research and Applications* **21**(5),894 (2013).
- [18] K. Kishore, P. Dwibedy, G. Dey, D. Naik, P. Moorthy, *Research on chemical intermediates* **24**(1),35 (1998).
- [19] R. Mane, B. Sankapal, C. Lokhande, *Materials research bulletin* **35**(4),587 (2000).
- [20] C.D. Lokhande, B.R. Sankapal, R.S. Mane, H.M. Pathan, M. Muller, M. Giersig, V. Ganesan, *Applied Surface Science* **193**(1-4),1 (2002).
- [21] A. Kariper, E. Guneri, F. Gode, C. Gumus, T. Ozpazan, *Mater Chem Phys* **129**(1-2),183 (2011).